WILEY-VCH

Edited by Mario Lanza

Conductive Atomic Force Microscopy

Applications in Nanomaterials

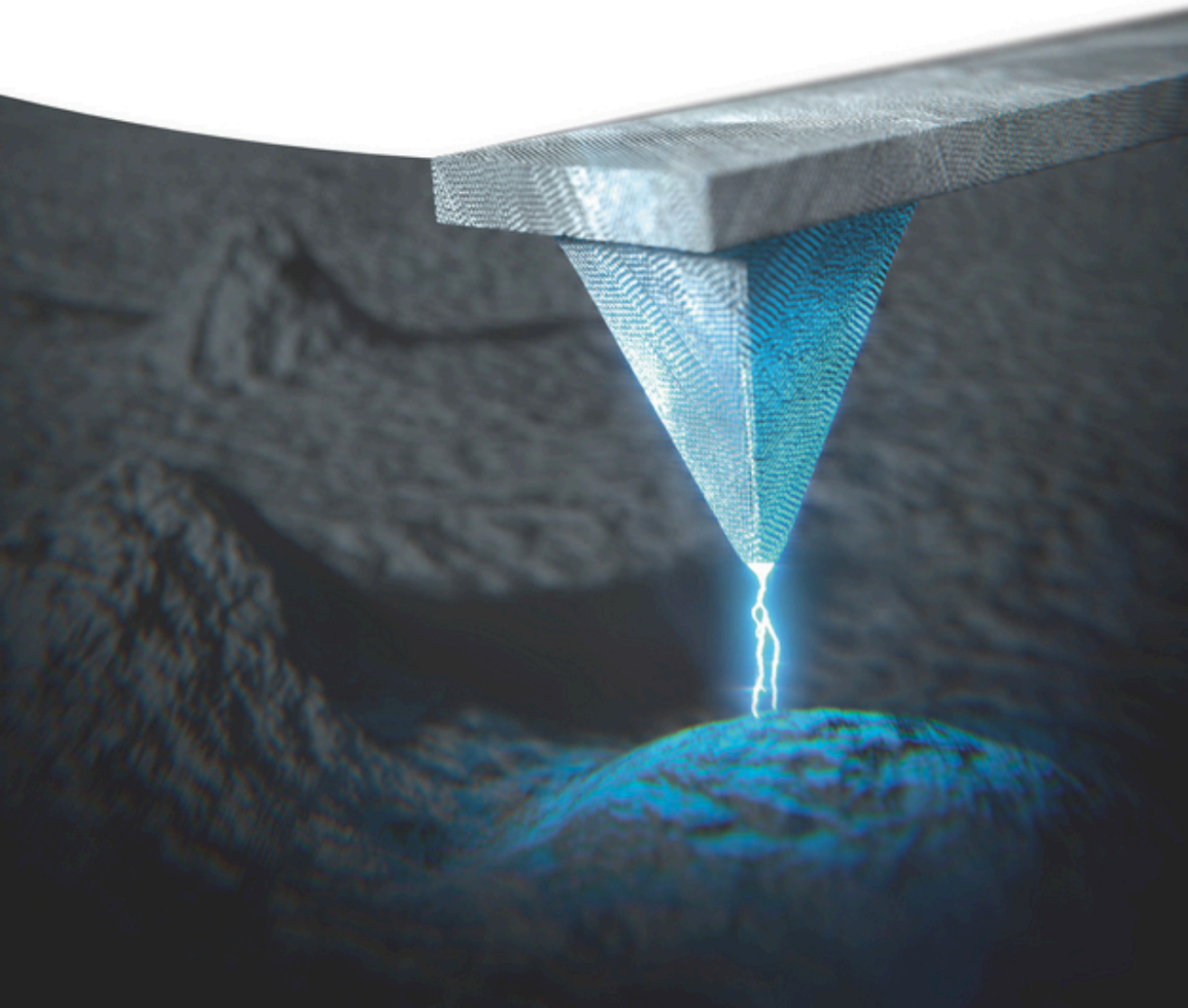

Conductive Atomic Force Microscopy

Conductive Atomic Force Microscopy

Applications in Nanomaterials

Edited by Mario Lanza

WILEY-VCH

Editor

Prof. Mario Lanza
Soochow University
Inst. of Funct. Nano & Soft Materials
199 Ren-ai Road
215123 Suzhou
China

Cover
Cover image was kindly provided by the editor

Library of Congress Card No.:
applied for

British Library Cataloguing-in-Publication Data
A catalogue record for this book is available from the British Library.

Bibliographic information published by the Deutsche Nationalbibliothek
The Deutsche Nationalbibliothek lists this publication in the Deutsche Nationalbibliografie; detailed bibliographic data are available on the Internet at <http://dnb.d-nb.de>.

Print ISBN: 978-3-527-34091-0
ePDF ISBN: 978-3-527-69978-0
ePub ISBN: 978-3-527-69979-7
Mobi ISBN: 978-3-527-69980-3
oBook ISBN: 978-3-527-69977-3

Cover Design Formgeber, Mannheim, Germany
Typesetting SPi Global, Chennai, India
Printing and Binding

Printed on acid-free paper

Contents

Oxide Films and Conduction AFM

Sean Joseph O'Shea

*A*STAR, Institute of Materials Research and Engineering (IMRE), Materials Processing and Characterization Department, 2 Fusionopolis Way, Singapore 138634, Singapore*

Conduction through oxides has always been part of the scanning probe microscopy (SPM) story. Indeed, the idea of the scanning tunneling microscope (STM) originates in part from how to locally study electrical properties of metal oxides [1]. However, a well-known limitation with STM is that it cannot be used on thick insulating surfaces, for which the sister technique atomic force microscopy (AFM) proved more practical in both research and industry.

One of the first SPM experiments on oxides was carried out by Mark Welland, in which he observed telegraph noise in thin SiO_2-on-Si with STM [2]. In early 1992, Martin Murrell joined Welland's STM group at Cambridge wanting to continue research on silicon oxides, especially the breakdown properties of very large-scale integration (VLSI) oxides. Given that the gate oxides at that time were far too thick (~10 nm) for STM, it was natural that attention turned to AFM. I was developing the AFM research in the group and Timothy Wong had constructed an all-digital SPM control system, which allowed great versatility in exploring different instrumentation methods. Jack Barnes and Sandy McKinnon provided much needed electrical engineering. Combining all this expertise, we implemented our version of Conductive atomic force microscopy (CAFM) by coating AFM cantilevers varnished with a 100-nm-thick film of titanium to make a conducting tip, programming the digital controller to output defined voltage ramps and limit the current flow to prevent catastrophic oxide breakdown, and then measuring current–voltage characteristics and images on 12-nm-thick, VLSI quality SiO_2 provided by Heyns and Verhaverbeke of IMEC [3].

The CAFM experiment worked without much trouble, and one of our conclusions, and indeed motivations, was that regions of the oxide could have far larger breakdown voltage than shown by conventional methods on large capacitor structures, presumably because the AFM probes nanoscale areas of the oxide, which are defect free. This conclusion was of course totally wrong! Our later work showed little difference between conventional device tests and CAFM [4]. It turned out a major issue was the applied electric field caused growth of material or contaminants under the tip, leading to higher than expected breakdown

voltages. This induced surface oxidation was an annoyance for electrical characterization efforts, but proved very useful as a novel direct write lithography method [5]. Actually, the research community pursuing nanoscale lithography was applying quite similar methodologies [6] and closely paralleled the activity in CAFM at the time.

The silicon tips used in our original work were also part of the problem. Gold wire tips and conducting diamond tips (developed by Philipp Niedermann from Neuchatel) were much more useful [4]. The problem of the tip, which remains a critical issue even today, arises from the very high mechanical and electrical stress experienced in CAFM at the tip–sample contact, leading to tip wear or local oxidation, and a protocol using simultaneous force curve and current measurement was proposed as a means to test the suitability of tips for CAFM [7]. Further studies, with Mark Lantz and Ken Johnson, highlighted the interplay between the measured conduction and the contact mechanics at nanometer length scales [8]. Subsequent approaches have extensively explored the use of intermittent or tapping mode CAFM to circumvent the problem of high forces acting on the tip.

In tandem with the aforementioned efforts in CAFM, other AFM-based approaches for nanoscale electrical characterization of semiconductor materials were being actively pursued, notably Kelvin Probe microscopy [9] and CAFM spreading resistance measurement [10], and the utility of CAFM and related AFM methods in semiconductor research remains strong. This is indicated by the many material systems studied over the last 20 years, ranging from nanoscale devices, single defects and dopants, dielectric and insulating thin films, quantum dots, nanowires, and 2D materials. The CAFM method has also found applications in "soft" matter materials, particularly in molecular electronics [11] and thin organic films [12]. An area that deserves more effort is application in biology, such as understanding charge transfer in photosynthesis or across lipid membranes. Here the challenges of working in aqueous environments while maintaining robust electrical measurement are daunting, but methods based on non-contact AFM, for example, Kelvin Probe, appear feasible.

I believe there will always be a need for characterization using conduction SPM methods because not only are real-world electrical devices and sensors becoming increasingly smaller, but at a fundamental level there is always a drive to further understand the basic building blocks of materials, that is, the functional and transport properties of materials at an atomic or molecular scale. This book brings together many of the SPM electrical characterization technologies and indicates future challenges and directions to explore, no doubt requiring further development of instrumentation and novel techniques. The continuing evolution of this research field is illustrated in a final example. We started our story developing CAFM because gate oxides were thick and STM could not be used. Some 20 years later, gate oxides are so thin that tunneling is possible across them and we now routinely use STM for gate dielectric studies. We have come full circle!

References

1 Binnig, G. and Rohrer, H. (1987) Scanning tunneling microscopy – from birth to adolescence. *Rev. Mod. Phys.*, **59** (3), 615–625.

2 Welland, M.E. and Koch, R.H. (1986) Spatial location of electron trapping defects on silicon by scanning tunneling microscopy. *Appl. Phys. Lett.*, **48** (11), 724–726.

3 (a) Murrell, M.P., Welland, M.E., O'Shea, S.J., Wong, T.M.H., Barnes, J.R., McKinnon, A.W., Heyns, M., and Verhaverbeke, S. (1993) Spatially resolved electrical measurements of SiO_2 gate oxides using atomic force microscopy. *Appl. Phys. Lett.*, **62** (7), 786–788;
(b) A similar idea was undertaken by Sugawara, Y., Fukano, Y., Nakano, A., Ida, T., and Morita, S. (1992) Oxidation site of polycrystalline silicon surface studied using scanning force/tunneling microscope (AFM/STM) in air. *Jpn. J. Appl. Phys.*, **31** (6A, Part 2), L725–L727.

4 O'Shea, S.J., Atta, R.M., Welland, M.E., and Murrell, M.P. (1995) Conducting AFM study of SiO_2 breakdown. *J. Vac. Sci. Technol. B*, **13**, 1945–1953.

5 (a) Snow, E.S. and Campbell, P.M. (1994) Fabrication of silicon nanostructures with an atomic force microscope. *Appl. Phys. Lett.*, **64** (15), 1932–1934;
(b) Day, H.C. and Allee, D.R. (1993) Selective area oxidation of silicon with a scanning force microscope. *Appl. Phys. Lett.*, **62** (21), 2691–2693.

6 (a) Mujumdar, A., Oden, P.I., Carrejo, J.P., Nagahara, L.A., Graham, J.J., and Alexander, J. (1992) *Appl. Phys. Lett.*, **61** (19), 2293–2295;
(b) Hosaka, S., Koyanagi, H., and Kikukawa, A. (1993) *Jap. J. Appl. Phys.*, **32** (3B, Part 2), L464–L467.

7 O'Shea, S.J., Atta, R.M., and Welland, M.E. (1995) Characterisation of tips for conducting AFM. *Rev. Sci. Instrum.*, **66**, 2508–2512.

8 Lantz, M.A., O'Shea, S.J., and Welland, M.E. (1997) Simultaneous force and conduction measurements in atomic force microscopy. *Phys. Rev. B*, **56**, 15345–15352.

9 Williams, C.C., Slinkman, J., Hough, W.P., and Wickramasinghe, H.K. (1989) Lateral dopant profiling with 200 nm resolution by scanning capacitance microscopy. *Appl. Phys. Lett.*, **55** (16), 1662–1664.

10 De Wolf, P., Snauwaert, J., Hellemans, L., Clarysse, T., Vandervorst, W., D'Olieslaeger, M., and Quaeyhaegens, D. (1995) Lateral and vertical dopant profiling in semiconductors by atomic force microscopy using conducting tips. *J. Vac. Sci. Technol. A*, **13** (3), 1699–1704.

11 Kelley, T.W., Granstrom, E.L., and Frisbie, C.D. (1999) *Adv. Mater.*, **11** (3), 261–264.

12 Specht, M., Ohnesorge, F., and Heckl, W.M. (1991) Simultaneous measurement of tunneling current and forces as a function of position through a lipid film on a solid substrate. *Surf. Sci.*, **257** (1–3), L653–L658.

List of Contributors

Fei Hui
Soochow University
Collaborative Innovation Center of Suzhou Nanoscience and Technology
Institute of Functional Nano & SoftMaterials (FUNSOM)
199 Ren-Ai Road
Suzhou 215123
China

Marco Allione
King Abdullah University of Science and Technology (KAUST)
Physical Science and Engineering Division (PSE)
SMILEs Lab
Thuwal 23955-6900
Saudi Arabia

Lidia Aguilera
Technology Transfer Company
Knowledge Innovation Market
08005 Barcelona
Spain

Guenther Benstetter
Deggendorf Institute of Technology
Faculty of Electrical Media and Computer Engineering
94469 Deggendorf
Germany

Patrizio Candeloro
University Magna Graecia
Departement of Experimental Clinics
Bionem Lab Campus "Salvatore Venuta" Viale Europa
88100 Germaneto-Catanzaro
Italy

Umberto Celano
KU Leuven
Department of Physics and Astronomy (IKS)
Celestijnenlaan 200D
3001 Leuven
Belgium

and

IMEC
Kapeldreef 75
3001 Heverlee (Leuven)
Belgium

Enzo Di Fabrizio
King Abdullah University of Science and Technology (KAUST)
Physical Science and Engineering Division (PSE)
SMILEs Lab
Thuwal 23955-6900
Saudi Arabia

and

University Magna Graecia
Departement of Experimental Clinics
Bionem Lab Campus "Salvatore Venuta" Viale Europa
88100 Germaneto-Catanzaro
Italy

Rimma Dekhter
Nanonics Imaging Ltd
Jerusalem
Israel

Patrick Fiorenza
Consiglio Nazionale delle Ricerche
Istituto per la Microelettronica e Microsistemi (CNR-IMM)
Strada VIII, 5
95121 Catania
Italy

Gabriele Fisichella
Consiglio Nazionale delle Ricerche
Istituto per la Microelettronica e Microsistemi (CNR-IMM)
Strada VIII, 5
95121 Catania
Italy

Werner Frammelsberger
Deggendorf Institute of Technology
Faculty of Mechanical Engineering and Mechatronics
Dieter-Görlitz-Platz 1
94469 Deggendorf
Germany

Filippo Giannazzo
Consiglio Nazionale delle Ricerche
Istituto per la Microelettronica e Microsistemi (CNR-IMM)
Strada VIII, 5
95121 Catania
Italy

Andrea Giugni
King Abdullah University of Science and Technology (KAUST)
Physical Science and Engineering Division (PSE)
SMILEs Lab
Thuwal 23955-6900
Saudi Arabia

Giuseppe Greco
Consiglio Nazionale delle Ricerche
Istituto per la Microelettronica e Microsistemi (CNR-IMM)
Strada VIII, 5
95121 Catania
Italy

Joan Grifoll-Soriano
Technology Transfer Company
Knowledge Innovation Market
08005 Barcelona
Spain

Enric Grustan-Gutierrez
Soochow University
Collaborative Innovation Center of Suzhou Nanoscience and Technology
Institute of Functional Nano & Soft Materials (FUNSOM)
199 Ren-Ai Road
Suzhou 215123
China

Alexander Hofer
Deggendorf Institute of Technology
Faculty of Electrical Media and Computer Engineering
94469 Deggendorf
Germany

Vanessa Iglesias
International Iberian Nanotechnology Laboratory
Av. Mestre José Veiga
4715-330 Braga
Portugal

Andrey Ignatov
Nanonics Imaging Ltd
Jerusalem
Israel

Xu Jing
Soochow University
Collaborative Innovation Center of Suzhou Nanoscience and Technology
Institute of Functional Nano & Soft Materials (FUNSOM)
Suzhou 215123
China

Oliver Krause
Nanoworld Services GmbH
Schottkystraβe 10
91058 Erlangen
Germany

Sasha Krol
Nanonics Imaging Ltd
Jerusalem
Israel

Mario Lanza
Soochow University
Institute of Functional Nano & Soft Materials
Suzhou 215123
China

David Lewis
Nanonics Imaging Ltd.
Har Hotzvim Hi-Tech Park
Beit Bynet
Jerusalem 97775
Israel

Donping Liu
Dalian Nationalities University
School of Physics and Materials Engineering
Dalian, Development Zone
Dalian 116600
China

Matteo Lorenzoni
Campus de la Universitat Autònoma de Barcelona
Microelectronics Institute of Barcelona (IMB-CNM, CSIC)
NEMS & Nanofabrication group
E-08193 Bellaterra
Spain

Yi Lv
Fudan University
Department of Physics
Shanghai 200433
China

Nicolas F. Martinez
Concept Scientifique Instruments (CSI)
17 Avenue des Andes
Les Ulis 91940
France

Sean Joseph O'Shea
A*STAR, Institute of Materials Research and Engineering (IMRE)
Materials Processing and Characterization Department
2 Fusionopolis Way
Singapore 138634
Singapore

Louis Pacheco
Concept Scientifique Instruments (CSI)
17 Avenue des Andes
Les Ulis 91940
France

Chengbin Pan
Soochow University
Collaborative Innovation Center of Suzhou Nanoscience and Technology
Institute of Functional Nano & Soft Materials (FUNSOM)
199 Ren-Ai Road
Suzhou 215123
China

Mathias Rommel
Fraunhofer Institute for Integrated Systems and Device Technology IISB
Schottkystrasse 10
91058 Erlangen
Germany

Francesc Pérez-Murano
Campus de la Universitat Autònoma de Barcelona
Microelectronics Institute of Barcelona (IMB-CNM, CSIC)
NEMS & Nanofabrication group
E-08193 Bellaterra
Spain

Gerardo Perozziello
University Magna Graecia
Departement of Experimental Clinics
Bionem Lab Campus "Salvatore Venuta" Viale Europa
88100 Germaneto-Catanzaro
Italy

Kin Leong Pey
Singapore University of Technology and Design (SUTD)
Engineering Product Development (EPD)
Singapore 487372
Singapore

Fabrizio Roccaforte
Consiglio Nazionale delle Ricerche
Istituto per la Microelettronica e Microsistemi (CNR-IMM)
Strada VIII, 5
95121 Catania
Italy

Albena Paskaleva
Institute of Solid State Physics
Bulgarian Academy of Sciences
72 Tzarigradsko Chaussee
1784 Sofia
Bulgaria

Yuanyuan Shi
Soochow University
Collaborative Innovation Center of Suzhou Nanoscience and Technology
Institute of Functional Nano & Soft Materials (FUNSOM)
199 Ren-Ai Road
Suzhou 215123
China

Shubhakar Kalya
Singapore University of Technology and Design (SUTD)
Engineering Product Development (EPD)
Singapore 487372
Singapore

Bo Song
Soochow University
Suzhou Key Laboratory of Macromolecular Design and Precision Synthesis
Jiangsu Key Laboratory of Advanced Functional Polymer Design and Application
College of Chemistry
Chemical Engineering and Materials Science
Suzhou 215123
China

Alina Strinkovsky
Nanonics Imaging Ltd
Jerusalem
Israel

Bruno Torre
King Abdullah University of Science and Technology (KAUST)
Physical Science and Engineering Division (PSE)
SMILEs Lab
Thuwal 23955-6900
Saudi Arabia

Wilfried Vandervorst
KU Leuven
Department of Physics and Astronomy (IKS)
Celestijnenlaan 200D
3001 Leuven
Belgium

and

IMEC
Kapeldreef 75
3001 Heverlee (Leuven)
Belgium

Rong Wu
Fudan University
Department of Physics
Shanghai 200433
China

Yijun Xia
Soochow University
Suzhou Key Laboratory of Macromolecular Design and Precision Synthesis
Jiangsu Key Laboratory of Advanced Functional Polymer Design and Application
College of Chemistry
Chemical Engineering and Materials Science
Suzhou 215123
China

Fei Xue
Fudan University
Department of Physics
Shanghai 200433
China

Xinju Yang
Fudan University
Department of Physics
Shanghai 200433
China

Shengli Zhang
Fudan University
Department of Physics
Shanghai 200433
China

Yifei Zhang
Fudan University
Department of Physics
Shanghai 200433
China

1

History and Status of the CAFM

Chengbin Pan, Yuanyuan Shi, Fei Hui, Enric Grustan-Gutierrez, and Mario Lanza

Soochow University, Collaborative Innovation Center of Suzhou Nanoscience and Technology, Institute of Functional Nano & Soft Materials (FUNSOM), 199 Ren-Ai Road, Suzhou 215123, China

1.1 The Atomic Force Microscope

The atomic force microscope (AFM, Figure 1.1) measures the interaction force that appears between an ultrasharp tip and a sample when the distance separating them is in the nanometric range [1]. The tip, which at the apex has a radius down to few nanometers, is located at the end of a cantilever. Its length, width, and thickness are typically of hundreds, tens, and few micrometers (respectively) [2]. The interaction force between the tip and the sample (F_c) produces a deflection of the cantilever according to Hooke's law [3] (see Eq. (1.1)), where k_c and δ_c are the spring constant and the deflection of the cantilever.

$$F_c = -k_c \cdot \delta_c \tag{1.1}$$

In most AFMs, this deflection is detected using an optical system based on a laser beam focused on the top surface of the cantilever driving the reflection to the center of a photodiode (see Figure 1.2) [4]. When the tip is far from the surface, the interaction between tip and sample is null and, therefore, no deflection of the cantilever is observed (the laser spot stays at the center of the photodiode). When the tip is close enough to the sample, the cantilever flexes due to the interaction force that appears between both of them, and the laser spot is deflected, changing its position on the photodiode. By processing the position of the laser spot on the photodiode, the force that has provoked such deflection can be quantified. Since the force depends on the distance that the tip has deflected (Eq. (1.1)), information about the topography of the analyzed sample can be obtained. Following this working principle, if the AFM tip is moved laterally along the surface of the sample (in the X and Y axes), topographic information about an entire area (many point locations) can be collected. These data are sent to the computer which, using an image processing software, can depict a three-dimensional (3D) topographic map [5]. Usually a standard AFM topographic map contains a matrix of 256×256 pixels (positions). The number of lines per image and pixels per line, as well as many other live scan parameters, such as tip lateral speed, can be easily modified via software.

Conductive Atomic Force Microscopy: Applications in Nanomaterials, First Edition.
Edited by Mario Lanza.

Figure 1.1 Photograph of the dimension icon AFM from Bruker. This is the most representative image of an AFM, as this equipment (and previous models with very similar structure) are by far the most widespread (sold) AFM configuration. (Reproduced with permission from [1]. Copyright Bruker 2015.)

However, this methodology entails certain risks: if the tip scans at a constant height in the Z-axis the presence of a high hillock on the surface of the sample can result in a dramatic collision, leading to unwanted tip/sample damage. Similarly, if the tip encounters a deep enough valley on the sample, the distance between them may become too large, leading to negligible tip/sample interaction and therefore failure to monitor the topography of the sample. To avoid these problems, the AFM uses an electronic feedback (controller) that continuously corrects the tip-to-sample distance in the Z-axis after measuring the height of each pixel (location) within the image (map), ensuring constant cantilever deflection during the whole scan [3] (see Figure 1.2). The cantilever deflection (also called the *deflection setpoint*) can be set by the user via software, and it controls the interaction force between the tip and the sample. The movement of

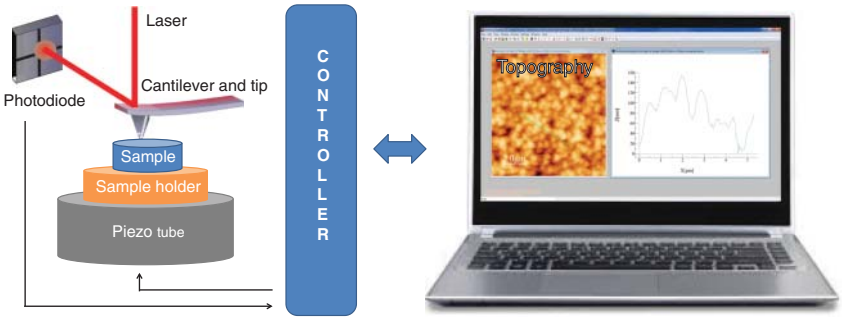

Figure 1.2 Schematic displaying how the cantilever deflections in an AFM can be processed to obtain a topographic map. The deflection of the cantilever is detected with a laser, and the changes of the laser position in the photodiode are sent to the controller which corrects the position of the tip through the piezo tube. The data are used to build a topographic map using an image processing software compatible with AFMs. (Modified and reprinted with permission from [4], copyright by Jelena Živković 2013.)

the tip and/or sample in the X, Y, and Z directions is normally applied through piezoelectric actuators. Most AFMs incorporate a piezotube that provides 3D movement to the tip and/or the sample (in Figure 1.2 it moves the sample). The AFM also requires a mechanical anti-vibration system that isolates it from external perturbations. This allow the AFM achieving a resolution down to 1 nm in the X, Y-directions and 0.1 nm in the Z-direction.

It is worth noting that some modern AFMs do not use an optical system (laser plus photodiode) to detect the changes on the tip deflection, instead they use a piezoelectric sensor attached to the cantilever. When the cantilever flexes, the resistance of the piezoelectric sensor changes quantifying the surface height. This system, called *tuning fork* [6], avoids mounting any hardware above the tip (e.g., photodiode) leading to an easy combination with other tools (e.g., Raman spectroscopy), as well as multiprobe configurations. This setup is analyzed in depth in Chapter 13.

Depending on the tip-sample distance during the measurements, different operation regimes can be described. For distances larger than 0.5 nm, the detected forces are mainly electrostatic, magnetic, and van der Waals, which result in an attractive regime [7, 8]. On the contrary, for distances smaller than 0.3 nm, the tip-sample interaction turns into a repulsive regime, in which it can be considered that the tip physically contacts the sample. The contact area between the tip and the sample (A_c) mainly depends on the contact force, the geometry of the tip, and the stiffness of both tip and sample, and it is widely accepted that it can range between 1 and 800 nm^2 [9, 10] (see also Chapter 3). Both operation regimes lead to the two classic operation modes of an AFM: the contact and the noncontact modes. The main difference between them is that in contact mode the vertical resolution is higher but, on the other hand, the lateral frictions with the surface of the sample are much larger, leading to undesired tip and/or sample wearing. Some alternative operation modes that combine the benefits from both of them (e.g., the tapping mode) [11] have been developed.

Finally, it is important to take into account that, when the AFM measurements are performed in air (without any environmental control system), a water layer gets deposited on the surface of both the tip and the sample owing to the ambient humidity. This water layer, which acts as a meniscus when the tip contacts the surface, introduces capillary forces between the tip and the sample, which must be also considered [12].

1.2 The Conductive Atomic Force Microscope

The conductive AFM (CAFM), also referred to in the literature as C-AFM, conductive probe AFM (CP-AFM), conductive scanning probe microscope (C-SPM), or conductive scanning force microscope (C-SFM), is basically an AFM that records the currents flowing at the tip/sample nanojunction simultaneously to the topography. The structure of a CAFM (see Figure 1.3) is very similar to that of the standard AFM, with only three main differences: (i) the probe tip must be conductive, (ii) a voltage source is needed to apply a potential difference between the tip and the sample holder, and (iii) a preamplifier is used to convert the (analogical) current signal into (digital) voltages that can be read by the computer. CAFM probes can be easily acquired from any manufacturer at competitive prices [2], the voltage source is located inside the AFM controller (no additional hardware is required), and the preamplifier can be purchased from the AFM manufacturer. In CAFM experiments, the sample is usually fixed on the sample holder using a conductive tape or paste, the most widely used being silver paints [13]. A Faraday cage is also convenient to isolate the sample from any external electrical interference. Using this setup, when a potential difference is imposed between the tip and the sample an electrical field is generated, which results in a net current flowing from the tip to the sample or vice versa. Therefore, the local electrical properties of the samples can be monitored at a very high nanometric resolution. The currents collected by the CAFM obey Eq. (1.2) [14], in which I is the total current flowing through the tip/sample nanojunction, J is the current density, and A_{eff} is the effective emission area

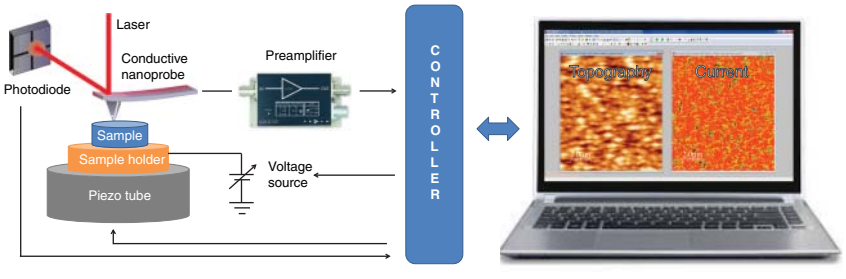

Figure 1.3 Block diagram of a conventional conductive atomic force microscope. Compared to the AFM, the three new elements are the conductive tip, preamplifier, and sample bias.

through which electrons can flow (from now on we will refer to it just as effective area).

$$I = J \cdot A_{\text{eff}} \tag{1.2}$$

The value of J mainly depends on the conductivity of the tip/sample system and the voltage applied between them, and it is highly affected by intrinsic inhomogeneities in the samples, such as thickness fluctuations, local defects, and doping. The lateral resolution of the technique is defined by the term A_{eff}, which can range from tenths of square nanometers up to thousands of square micrometers depending on many experimental factors, including the conductivity of the sample, the geometry of the tip, the tip/sample contact force, the stiffness of the tip and the sample, and even the relative humidity of the atmosphere in which the experiment is performed.

The most common mistake in CAFM research is to assume that the effective emission area (A_{eff}) equals the physical contact area (A_c). Strictly, this assumption is erroneous because in many different tip/sample systems, the electrical field applied may propagate laterally (see Figure 1.4). For example, when the CAFM tip is placed on a metallic electrode, A_{eff} equals the entire area covered by the electrode, as its lateral electrical conductivity is very high [15, 16]. In order to provide a comprehensive definition, the effective area A_{eff} can be understood as the sum of all those infinitesimal spatial locations on the surface of the sample that are electrically connected to the CAFM tip (the potential difference is negligible). As such, A_{eff} is a virtual entity that summarizes all electrically relevant effects within the tip/sample contact system into a single value, over which the current density is assumed to be constant. The difference between contact area and effective emission area is explained in depth in Chapters 3 and 4. The small

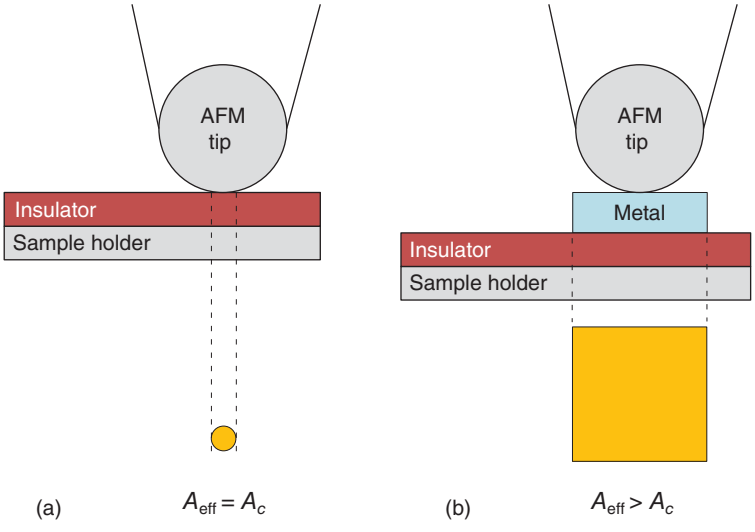

Figure 1.4 Schematic of the effective emission area through which electrons can flow (A_{eff}) in a CAFM when the tip is placed on (a) a flat insulating sample and (b) a flat metallic electrode deposited on an insulating sample.

dimensions of A_{eff} make the current densities flowing through the tip/sample system extremely large. The smallest currents detected by a CAFM are defined by its electrical noise, which is (in the best cases) hundreds of femtoamperes. A 1 pA current flowing through a typical A_{eff} of 100 nm^2 gives a current density of 1 A/cm^2. Such large current densities can dramatically accelerate the degradation of most CAFM probe tips, reducing the reliability of the measurements and increasing the cost of the research. This problem is further aggravated by the high lateral frictions present in the tip/sample system during the scans [17, 18].

The first types of conductive nanoprobes used in CAFM experiments, which are still widely used nowadays, are the standard silicon nanoprobes varnished with thin metallic films, including Pt, Au, Ru, Ti, and/or Cr (Figure 1.5). The thickness of the varnish should be thick enough to withstand the large current densities and frictions, and at the same time thin enough to not increase significantly the radius of the tip apex, maintaining its sharpness and ensuring a high lateral resolution during the measurements. As mentioned, the lifetime of conductive tips for CAFM experiments is much shorter than in any other AFM mode, mainly owing to metallic varnish melting and loss of tip mass during the scans. To solve this problem, new CAFM silicon tips coated with hard materials (e.g., phosphorous-doped diamond [19] and graphene [17, 18, 20–24]), as well as full conductive tips [25–27] have appeared (see Figure 1.5). Other factors related to the sample, such as stiffness, rugosity, stickiness, and conductivity play very important roles when deciding on the type of tip to be used in a CAFM analysis. Chapter 2 presents an in-depth description of the fabrication process and reliability of conductive nanoprobes for AFM. Advices on how to select the best CAFM tip for each experiment are provided in Chapter 2.

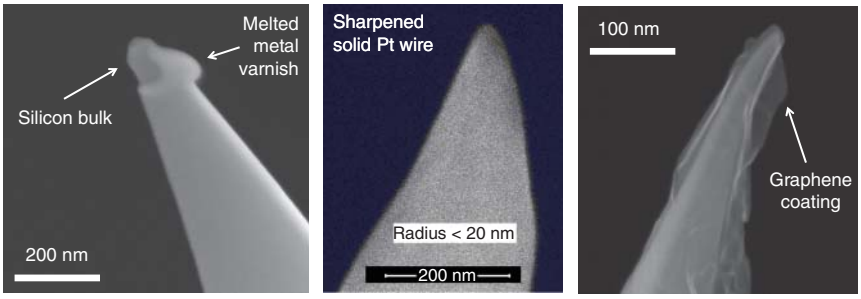

Figure 1.5 (a) Scanning electron microscope images of (a) metal-varnished silicon nanoprobe, (b) a sharpened solid Pt wire compatible for CAFMs, and (c) a metal-varnished silicon nanoprobe coated with a sheet of single-layer graphene. The picture in (a) intentionally shows a tip with the metallic varnish worn off, so that the core bulk of silicon can be observed. (Panels (a) and (c) have been modified and reprinted with permission from [18], copyright from Royal Society of Chemistry 2016. Panel (b) has been reproduced with permission from [25], copyright American Institute of Physics 2004.)

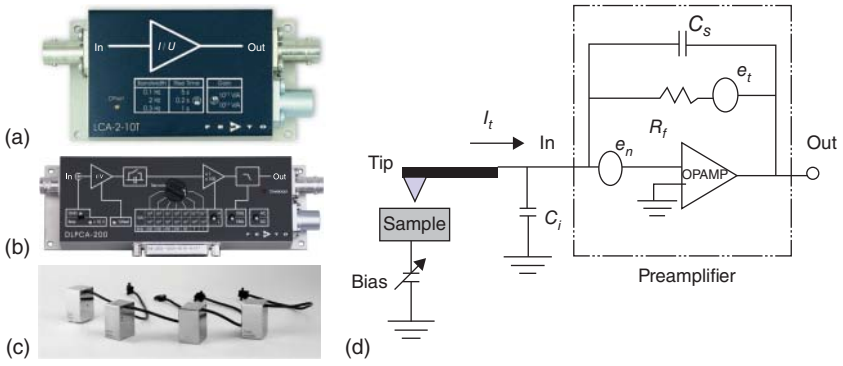

Figure 1.6 (a, b) Photographs of two preamplifiers for CAFMs, the first one with fixed gain and the second with variable gain. (c) Photographs of different application modules for Bruker AFMs, including the CAFM module (which contains a preamplifier). (d) Simplified schematic of a conventional preamplifier used in CAFMs. The main parts are (i) an operational amplifier with high input impedance (OPAMP); (ii) a feedback resistor (R_f) and its parasite capacitor (C_s) and Johnson noise (e_t)-associated effects; (iii) a noise voltage source associated with the operational amplifier (e_n); and (iv) a capacitance associated with the input interconnections (C_i). (Panels (a) and (b) have been reprinted from [29], copyright FEMTO 2015. Panel (d) has been modified and reprinted with permission from [30], copyright American Institute of Physics 1990.)

The analogical current signals flowing through the tip/sample nanojunction are sent to the preamplifier Figure 1.6a,b, which transforms them into digital voltages that can be read by the data acquisition (DAQ) card of the computer (see Figure 1.6). Many manufacturers integrate the preamplifier in the so called "CAFM application module," which is a removable component that can be fixed to the AFM (usually very close to the tip to minimize electrical noise). Similarly, many other modules allow AFMs to perform other operations (see Figure 1.6c), such as scanning capacitance microscopy (SCM) or scanning spreading resistance microscopy (SSRM). In most CAFM experiments, the currents measured can range typically from few picoamperes to hundreds of microamperes, while the voltages readable by the DAQ card usually range between −3 and +3 V [31]. Therefore, the preamplifier needs to provide a very low noise and a high transimpedance (gain). Figure 1.6d shows the simplified schematic of a typical low-noise preamplifier for CAFM measurements [30], in which some elements can be distinguished: (i) an operational amplifier with high input impedance; (ii) a feedback resistor (R_f) and its parasite capacitor (C_s) and Johnson noise (e_t)-associated effects; (iii) a noise voltage source associated with the operational amplifier (e_n); and (iv) a capacitance associated with the input interconnections (C_i). A correct selection of the electrical components is essential to achieve good and reliable CAFM data acquisition. For example, the value of R_f is not trivial: a very high value of R_f improves the noise-signal ratio, while reduces the bandwidth of the preamplifier. Therefore, the value of R_f should

be chosen to provide enough bandwidth and a noise level below the current values that we want to measure. The parameter e_n can be easily reduced by using a commercial low-noise operational amplifier. The capacitance associated with the connections (C_i) can be easily minimized by placing the preamplifier as near as possible to the conductive tip. The company FEMTO, one of the world's leading manufacturers of preamplifiers compatible with CAFMs, can provide devices with electrical noise as low as 3 fA and a gain up to 10^{13} V/A [29] (similar to those in Figures 1.6). Nevertheless, the main limitation of CAFM preamplifiers is their narrow current dynamic range, which usually allows collecting electrical signals only within three or four orders of magnitude (or even less). To solve this problem, preamplifiers with an adjustable gain can be used to focus on specific ranges [29] (similar to the one in Figure 1.6b). A more sophisticated solution for this problem is to combine the CAFM with a sourcemeter [17, 18], semiconductor parameter analyzer (SPA), or with a logarithmic preamplifier [28], which can capture the currents flowing through the tip/sample system at any range and with a high resolution. These methodologies are amply described in Chapters 10–12.

The currents flowing through the tip/sample system and converted by the preamplifier are (in almost every CAFM experiment) a consequence of the application of a voltage between the tip and the sample holder. Only a small portion of the works reported with CAFM did not require the application of a bias, that is, in the case of experiments in which the current is generated by other means, such as photoelectric [32] or piezoelectric [33] effects. Most CAFMs let the user select the value and polarity of the bias which should be applied on the tip while keeping the sample holder grounded, or vice versa. Therefore, the currents usually flow vertically through the sample [10], although lateral currents can be also measured by connecting the surface of the sample to the sample holder [34] (e.g., using silver paint or a wire bonder). Usually CAFM electronics allow applying voltages ranging from −10 to +10 V and, as mentioned, the currents that can be observed are always within three or four orders of magnitude, never smaller than 1 pA or larger than 10 μA. Apart from constant voltage stresses (CVS) applied during a scan, ramped voltage stresses (RVS) to collect current versus voltage (I–V) curves can also be performed by keeping the tip static at one single location (during the RVS). Despite this setup being more than enough for many experiments, some studies may require the use of enhanced electronic capabilities, such as the application of constant current stresses (CCS), the measurement of current versus time curves (I–t), the use of current limitations, or simply the application or measurement of larger voltages or currents. Many AFMs incorporate an input/output directly connected to the tip or the sample holder (or even both), allowing the use of an external sourcemeter or an SPA to apply/collect electrical signals. A detailed description of the combination of CAFM with a sourcemeter and SPA is presented in Chapter 10.

With this setup, many different kinds of experiments have been performed in recent years. The CAFM can be used to monitor the properties of materials, as well as to modify them with atomic resolution.